THE JOURNAL OF BIOLOGICAL CHEMISTRY VOL. 282, NO. 20, pp. 14923–14931, May 18, 2007

Thyroid Transcription Factor-1 Facilitates Cerebrospinal Fluid Formation by Regulating Aquaporin-1 Synthesis in the Brain*

Received for publication, February 16, 2007, and in revised form, March 19, 2007 Published, JBC Papers in Press, March 19, 2007, DOI 10.1074/jbc.M701411200

Jae Geun Kim[‡1], Young June Son[‡1], Chang Ho Yun[‡1], Young Il Kim[§], Il Seong Nam-goong[§], Jun Heon Park[‡2], Sang Kyu Park[¶], Sergio R. Ojeda[‖3], Angela Valentina D'Elia[4], Giuseppe Damante[**4], and Byung Ju Lee[‡5]**

*From the [‡]Department of Biological Sciences, College of Natural Sciences, University of Ulsan, Ulsan 680-749, South Korea, the [§]Department of Internal Medicine and [¶]Department of Pediatrics, Ulsan University Hospital, Ulsan 682-060, South Korea, the [‖]Division of Neuroscience, Oregon National Primate Research Center/Oregon Health and Science University, Beaverton, Oregon 97006, and the **Department of Biomedical Sciences and Technologies, University of Udine , 33100 Udine, Italy*

In the brain, aquaporin-1 (AQP-1), a water channel for high osmotic water permeability, is mainly expressed in the apical membrane of the ventricular choroid plexus and regulates formation of cerebrospinal fluid (CSF). Although the physiology of AQP-1 has been the subject of several publications, much less is known about the trans-acting factors involved in the control of *AQP-1* gene expression. Here we report that TTF-1, a homeodomain-containing transcriptional regulator, is coexpressed with AQP-1 in the rat brain choroid plexus and enhances *AQP-1* gene transcription by binding to conserved core TTF-1-binding motifs in the 5′-flanking region of the *AQP-1* gene. Intracerebroventricular administration of an antisense TTF-1 oligodeoxynucleotide significantly decreased AQP-1 synthesis and reduced CSF formation. In addition, blockade of TTF-1 synthesis increased survival of the animals following acute water intoxication-induced brain edema. These results suggest that TTF-1 is physiologically involved in the transcriptional control of AQP-1, which is required for CSF formation.

Cerebrospinal fluid (CSF),[6] a major constituent of the extracellular fluid in the central nervous system, fills the ventricles of the brain, spinal canal, and subarachnoid space. Most CSF in the cerebral ventricular system is formed in discrete sites, including the choroid plexus and circumventricular organs of the lateral, third, and fourth ventricles. Altogether, these sites produce nearly 90% of all ventricular CSF (1).

CSF has several important functions. Foremost, it provides a mechanical cushion to protect the brain from impact with the bony calvarium when the head moves (2) and also serves as a flexible physical support for the brain. In addition, it facilitates the transport of nutrients, peptides, and hormones into the brain. Because CSF communicates with the interstitial fluid of the brain, it plays an important role in maintaining a constant external environment for neurons and glia (3).

Regulation of brain water content and brain volume is critical for normal functioning of the central nervous system, which is highly sensitive to any change in fluid osmolality. Aquaporins (AQPs), a family of small integral membrane proteins, have been implicated in the regulation of water homeostasis in the brain (4). Numerous studies have shown that the expression of AQP-1, -4, and -9 is sensitive to brain injury, swelling, and other experimental interventions that affect the homeostatic regulation of brain water balance (5–7). AQP-1, a water channel for high osmotic water permeability, is abundantly present in the epithelium of kidney, lung, eye, liver, and brain (8). AQP-1 was first discovered in human erythrocytes (9). In the brain, AQP-1 is mainly expressed in the apical (CSF-facing) membrane of the ventricular choroid plexus epithelium and regulates the formation of CSF (10, 11). The mechanisms underlying the transcriptional control of AQP-1 gene expression in the brain, however, are poorly understood.

We report that thyroid transcription factor-1 (TTF-1), a homeodomain-containing transcription factor, regulates AQP-1 gene transcription in the choroid plexus. TTF-1 was first identified in the thyroid gland (12), and its cDNA was cloned and characterized as having sequence homology with the *Drosophila* NKx-2 homeodomain transcription factor (13). A different study identified the lung and fetal diencephalon as additional sites of TTF-1 expression (14). We and others have reported that TTF-1 remains expressed in the discrete regions of the postnatal rat brain (15, 16). More recently, we showed that TTF-1 is expressed in the subfornical organ where it regulates angiotensinogen synthesis (17).

During the course of these experiments, we noticed the presence of TTF-1 mRNA in the rat choroid plexus, and thus we examined the 5′-flanking region of the AQP-1 gene; we found several conserved core TTF-1-binding motifs. Promoter analy-

* This work was supported in part by Korea Research Foundation Grant KRF-2002-015-CS0045. The costs of publication of this article were defrayed in part by the payment of page charges. This article must therefore be hereby marked "*advertisement*" in accordance with 18 U.S.C. Section 1734 solely to indicate this fact.

[1] Supported in part by Neurobiological Research Fund B020203 and Brain Korea 21 grant.

[2] Worked as a volunteer for this study. Present address: University of Washington, Seattle, WA 98105.

[3] Supported by National Institutes of Health Grants HD25123, RR00163, and U54 HD18185 through cooperative agreement as part of the Specialized Cooperative Center Program in Reproduction Research.

[4] Supported by a Cofinanziamento Progetti di Ricerca di Rilevante Interesse Nazionale from Ministero dell'Università e della Ricerca.

[5] To whom correspondence should be addressed. Tel.: 82-52-259-2351; Fax: 82-52-259-1694; E-mail: bjlee@ulsan.ac.kr.

[6] The abbreviations used are: CSF, cerebrospinal fluid; AQP-1, aquaporin-1; TTF-1, thyroid transcription factor-1; AS, antisense; ODN, oligodeoxynucleotide; FISH, fluorescence *in situ* hybridization; RT, reverse transcription; DIG, digoxygenin; PBS, phosphate-buffered saline; HRP, horseradish peroxidase; TTF-1 HD, TTF-1 homeodomain; EMSA, electrophoretic mobility shift assay; SCR, scrambled; FITC, fluorescence isothiocyanate; ICP, intracranial pressure; dDAVP, 1-deamino-8-D-arginine vasopressin; AS, antisense.

sis performed in the BAS8.1 (astrocyte) and C6 (glioblastoma) cell lines showed that TTF-1 activated AQP-1 transcription in a dose-dependent manner. Electrophoretic mobility shift assays showed that TTF-1 bound specific subsets of putative DNA recognition sites in the AQP-1 promoter. *In vivo* experiments in which inhibition of TTF-1 synthesis was achieved by administration of antisense (AS) oligodeoxynucleotide (ODN) into the lateral ventricle decreased AQP-1 synthesis and, in turn, led to a decrease in CSF formation.

EXPERIMENTAL PROCEDURES

Animals and Tissue Preparation—Two-month-old male Sprague-Dawley rats (Daehan Animal Breeding Co., Chungwon, Korea) were used in this study. Following arrival, rats were housed in a room with a conditioned photoperiod (12-h light/12-h darkness, lights on from 600 to 1800 h) and temperature (23–25 °C) and allowed *ad libitum* access to tap water and pelleted rat chow. Animals were sacrifice, and the choroid plexus was collected from their brains. The tissues were quickly frozen on dry ice and stored at −80 °C until RNA or protein isolation was performed. Some brain samples were placed in embedding medium (Tissue-Tek, Torrance, CA) and frozen by placing them in 2-methylbutane (isopentane) immersed in liquid nitrogen for 2 min and then stored in a −80 °C freezer for cryosectioning at a later time. Twelve-μm cryostat sections were prepared, maintaining the cryostat temperature at −20 °C, and were mounted onto SuperFrost slides (Fisher). The slides were kept at −80 °C until used for fluorescence *in situ* hybridization (FISH).

PCR Cloning of TTF-1 and AQP-1 cDNA Fragments and 5′-Flanking Region of the AQP-1 Gene—A cDNA fragment derived from TTF-1 mRNA was cloned by reverse transcription (RT)-PCR from rat hypothalamic RNA. The specific primer sets (sense primer, 5′-AAC AGT CAA GCA AAT CCA AC-3′; antisense primer, 5′-AAT ACC AAA CCG TGG AGT AA-3′) were designed to generate a 552-bp TTF-1 cDNA fragment corresponding to nucleotides 1669–2220 in rat TTF-1 mRNA (NCBI GenBank™ accession number X53858). A rat AQP-1 cDNA fragment was also cloned by RT-PCR from rat choroid plexus RNA. The specific primer set (sense primer, 5′-AGC GAA ATC AAG AAG AAG C-3′; antisense primer, 5′-ATA TCA TCA GCA TCC AGG TC-3′) generates a 773-bp AQP-1 cDNA fragment corresponding to nucleotides 7–779 in rat AQP-1 mRNA (NCBI GenBank™ data base, accession number NM_012778). The cDNA fragments were cloned into a pEZ-T vector (RNA Corp., Seoul, Korea); constructs were confirmed by DNA sequencing. The proximal promoter of the human AQP-1 gene (−1779 to +22 bp) that was to be employed for promoter analysis was also cloned by PCR from human genomic DNA using the sequence information deposited in the NCBI GenBank™ data base (accession number AF026479). The sense primer was 5′-ACT TAT GAC CTT CGG CCA CC-3′, and the antisense primer was 5′-GGT GCT CAA TTC CCT CTG AG-3′. The 1802-nucleotide-long PCR product was inserted into a luciferase reporter plasmid (pGL-3 basic, Promega, Madison, WI), and its sequence was confirmed by DNA sequencing. Fourteen AQP-1 promoter constructs containing individually mutated core TTF-1-binding motifs were generated using the QuikChange™ site-directed mutagenesis kit (Stratagene, La Jolla, CA) according to the manufacturer's instructions; the intended mutations were confirmed by DNA sequencing.

Fluorescence in Situ Hybridization (FISH)—The TTF-1 cDNA template described above was linearized by SpeI and NcoI digestion for the production of either sense or antisense RNA probes, respectively, and the AQP-1 cDNA was linearized using either NotI or SalI. *In vitro* transcription of digoxygenin (DIG)-labeled or fluorescein-labeled cRNA probes was performed using an RNA labeling mix (Roche Applied Science) and T3 and T7 RNA polymerases (Promega).

Tissue sections were fixed with 3% paraformaldehyde in phosphate-buffered saline (PBS), pH 7.4, for 10 min. Following two 5-min washes with PBS, the slides were incubated in a 0.25% acetylation solution for 10 min to reduce ionic background. After acetylation, the sections were washed three times in 2× SSPE (pH 7.4, 0.3 M NaCl, 20 mM NaH_2PO4, 2 mM EDTA) for 5 min and dehydrated in ascending ethanol concentrations (75, 90, and 100%, 2 min each). To reduce nonspecific background, prehybridization was performed in hybridization buffer (50% formamide, 2× SSPE, 1× Denhardt's solution, 1 mg/ml yeast tRNA, 100 μg/ml polyadenylic acid, 500 μg/ml salmon sperm DNA, and 4 units/ml RNase inhibitor) at 60 °C for 3 h. The hybridization procedure was performed overnight at 60 °C using 200 μl of hybridization solution containing 300 ng of probe (a DIG-labeled cRNA probe to detect TTF-1 mRNA or a fluorescein-labeled cRNA probe to detect AQP-1 mRNA). The next morning the sections were incubated in 50% formamide and 2× SSPE at 62 °C for 1 h and washed with 0.2× SSPE and 0.1× SSPE (30 min each) at 62 °C. After the last washing step, to reduce endogenous peroxidase activity, the slides were incubated with 1% H_2O_2 in TNT buffer (0.1 M Tris-HCl, pH 7.5, 0.15 M NaCl, 0.3% Triton X-100) for 30 min and washed three times with TNT buffer for 5 min each. A blocking step with TNB blocking buffer (0.1 M Tris-HCl, pH 7.5, 0.15 M NaCl, 0.5% Blocking Reagent (PerkinElmer Life Sciences)) for 1 h at room temperature was followed by 1 h of incubation with horseradish peroxidase (HRP)-conjugated anti-DIG antibody (a final concentration of 1.5 milliunits/ml; Roche Applied Science) or with HRP-conjugated anti-fluorescein antibody (0.75 milliunits/ml; Roche Applied Science) in TNB blocking buffer. After washing three times in TNT buffer for 5 min each, mRNA signals of TTF-1 and AQP-1 were detected by using a Cy3-labeled and FITC-labeled tyramide signal amplification system, respectively (PerkinElmer Life Sciences).

Simultaneous Detection of TTF-1 and AQP-1 Transcripts Using Double FISH—To visualize mRNA expression of these two genes, sections were hybridized simultaneously with a DIG-labeled TTF-1 cRNA probe and a fluorescein-labeled AQP-1 cRNA probe. The detailed procedure for detection of each probe is described above. Briefly, the DIG-labeled TTF-1 probe was detected by incubating with HRP-conjugated DIG antibody (anti-DIG-HRP). After incubation with Cy3-coupled tyramide to detect the DIG-labeled TTF-1 probe, the sections were washed three times in TNT buffer for 5 min each. To quench the peroxidase activity of anti-DIG-HRP, the sections were incubated with 2% H_2O_2 in TNT buffer for 2 h and washed

three times in TNT buffer for 5 min each. To detect fluorescein-labeled AQP-1 probe, sections were then placed in TNB blocking buffer for 1 h at room temperature and incubated with HRP-conjugated anti-fluorescein antibody for 1 h. After washing three times in TNT buffer for 5 min each, signals were detected by incubating with FITC-coupled tyramide. Finally, the slides were dipped in Hoechst 33258 (Sigma) solution for visualization of cell nuclei.

Microscopy and Imaging—FISH images were captured with an InfinityX CCD camera (Lumenera Corp., Ontario, Canada) attached to an Axioskop2 Plus fluorescence microscope (Zeiss, Thornwood, NY). Merged images were analyzed using i-solution (iMTechnology, Seoul, Korea) image processing software. The Cy3 fluorescence image was visualized with a 546-nm green excitation filter set. FITC signal was observed with a 450–490-nm blue excitation filter set. Hoechst 33258 fluorescence emission from cell nuclei was observed with a 365-nm excitation filter. In addition, confocal microscope images were acquired using a Fluoview FV500 confocal microscope (Olympus, Tokyo, Japan). Further image processing was carried out using Adobe Photoshop 7.0 software. No selective visual enhancement of specific area or cells was applied to the images.

Cell Culture and Assays for Luciferase Activity—BAS8.1 and C6 cells were grown in Dulbecco's modified Eagle's medium/F-12 medium containing 10% fetal bovine serum, and the cultures were maintained at either 34 °C (BAS8.1 cells) or 37 °C (C6 cells) in an atmosphere of 5% CO_2, 95% air. Twenty four h after seeding the cells in 12-well plates, they were transiently transfected with the AQP-1 promoter-luciferase reporter construct (AQP-1-P) using Lipofectamine (Invitrogen) along with different concentrations (100–400 ng/well) of the expression vector pcDNA 3.1-zeo (Invitrogen) containing the TTF-1 coding region (TTF-1-pcDNA) (15). Transfection efficiency was normalized by cotransfecting the β-galactosidase reporter plasmid (pCMV-β-gal; Clontech) at 20 ng/ml. Cells were harvested 24 h after transfection and used for both luciferase and β-galactosidase assays as described previously (18). Cells containing different combination of vectors were simultaneously cultured and assayed for each experiment. In each case, we used 6 wells per condition, and each experiment was repeated 2–3 times.

Electrophoretic Mobility Shift Assay (EMSA)—The procedure for expression and purification of the TTF-1 homeodomain (TTF-1HD) protein has been described previously (19). Double-stranded oligodeoxynucleotides 5′-labeled with ^{32}P were used as probes. Sequences of the oligodeoxynucleotides employed are shown in Table 1. Oligodeoxynucleotides C and Cβ were used as a positive and negative control, respectively (20). EMSA was performed as described previously (17, 18), using the TTF-1 HD and oligonucleotides at final concentrations of 150 and 5 mM, respectively. Electrophoretically separated signals corresponding to the protein-bound and free DNA were quantitated with Multianalyst software. Binding of TTF-1HD to the oligodeoxynucleotides representing different regions of the AQP-1 promoter was expressed as a percentage of TTF-1HD binding to oligodeoxynucleotide C, which contains the core TTF-1 binding domain and flanking region of the thyroglobulin gene promoter (12).

To determine endogenous binding activity of nuclear extracts from the choroid plexus to the TTF-1 binding domains in the 5′-flanking region of the AQP-1 gene, nuclear protein fractions from the rat choroid plexus were prepared according to the method of Andrews and Faller (21), utilizing the mixture of protease inhibitors recommended by Kuhn *et al.* (22). The binding assay was performed as described previously (17), using 15 μg of protein and 20,000 cpm of probe (−724 in Table 1). To further confirm the presence of immunoreactive TTF-1 in the nuclear extracts, the proteins were incubated with 1 μl of undiluted TTF-1 antiserum (NeoMarkers, Fremont, CA) or preimmune serum for 30 min at room temperature before initiating the binding reactions.

Intracerebroventricular Administration of AS TTF-1 ODN—To determine the effect of blocking TTF-1 expression on AQP-1 synthesis and formation of CSF, a phosphorothioate AS TTF-1 ODN (GenoTech Corp., Daejeon, Korea) was delivered into the lateral ventricle of adult male rats. The AS TTF-1 ODN used to disrupt TTF-1 synthesis (5′-GAC TCA TCG ACA TGA TTC GGC GTC-3′) was directed against the sequence surrounding the first ATG codon of TTF-1 mRNA as reported previously (17, 18). As a control, a scrambled (SCR) sequence of identical base composition was used (5′-AGT CCT ACT CGG TAC GTA TGC AGC-3′). For the intracerebroventricular injection, ODNs were diluted to a final concentration of 1 nmol/μl in artificial cerebrospinal fluid (in mM, 126 NaCl, 2.5 KCl, 1.24 NaH_2PO_4, 1.3 $MgSO_4$, 2.4 $CaCl_2$, 26 $NaHCO_3$, 10 D-glucose, pH 7.3, and bubbled with 95% air, 5% CO_2). Injections were performed under pentobarbital (7.5 mg/kg body weight) and ketamine hydrochloride (25 mg/kg body weight) anesthesia. A polyethylene cannula (outer diameter of 1.05 mm and inner diameter of 0.35 mm) containing an inner stylet was stereotaxically implanted into the brain with its opening protruding from the roof of the lateral ventricle (coordinates were as follows: antero-posterior = 1.0 mm caudal to the bregma; ventral = 3.6 mm from the dura mater; lateral = 0.16 mm from the mid-line). After a week of recovery, the inner stylet was removed, and the ODNs (4 μl) were injected twice with a Hamilton syringe at a 12-h interval. The animals were sacrificed 12 h after the second ODN administration, and total RNA and proteins were extracted from the choroid plexus of the lateral ventricle. Changes in CSF secretion were also measured in other animals 12 h after the second ODN injection.

Western Blots—Choroid plexus tissue from SCR or AS ODN-treated animals was homogenized in lysis buffer (T-PER tissue protein extract reagent; Pierce) containing a protease inhibitor mixture (1 mM phenylmethylsulfonyl fluoride, 10 μg/ml leupeptin, 3 mM aprotinin) and 1 mM sodium orthovanadate, pH 6.8. Electrophoretically separated polypeptides were transferred onto a nitrocellulose membrane at 20 mA for 16 h using transfer buffer (25 mM Tris, 192 mM glycine, and 20% methanol, pH 8.3). The nitrocellulose membrane was blocked with 1% bovine serum albumin in PBS. After incubation with a monoclonal mouse TTF-1 antibody (1:2000) (NeoMarkers) or a polyclonal goat AQP-1 antibody (1:5000) (Santa Cruz Biotechnology, Santa Cruz, CA) for 1 h, bound antibody was detected with an ECL detection kit (Amersham Biosciences), according to the

manufacturer's recommended protocol. The membranes were exposed to x-ray film for 5 min in a dark room.

Real Time PCR—Total RNA was isolated from the rat choroid plexus using TRIzol reagent (Sigma). Total RNA (2 μg) was reverse-transcribed and amplified by a real time PCR using two sets of primers as follows: AQP-1 sense primer, 5′-CATGTATATCATCGCGGAGT-3′, and antisense primer, 5′-CACAGCCAGTGTAGTCAATG-3′; glyceraldehyde-3-phosphate dehydrogenase sense primer, 5′-TGTGAACGGATTTGGCCGTA-3′, and antisense primer, 5′-ACTTGCCGTGGGTAGAGTCA-3′. Real time PCRs (20-μl total volume, containing 5 pmol of primer, 10 μl of SYBR green dye (Qiagen, Valencia, CA), and 2 μl of cDNA) were carried out in capillaries of a DNA Engine Opticon continuous fluorescence detection system (MJ Research Inc., Waltham, MA) for ~40 cycles.

Assays for CSF Production—CSF production was measured by the ventriculocisternal perfusion method as described previously (23). Animals who were intracerebroventricular-injected with ODNs were anesthetized with pentobarbital (7.5 mg/kg body weight) and ketamine hydrochloride (25 mg/kg body weight), placed on a stereotaxic device, and subjected to catheterization of the lateral ventricle and the cisterna magna. Lateral ventricles of the brain were perfused with artificial cerebrospinal fluid containing 1 mg/ml fluorescence isothiocyanate (FITC)-dextran (M_r 70,000) as a volume marker (7) at 4 μl min^{-1} using a slow drive syringe pump (KDS 100, *kd*Scientific, Holliston, MA). CSF samples from the cisterna magna were collected at 10-min intervals for 90 min. Fluorescence from the collected CSF samples was measured in a fluorescence spectrophotometer (Wallac Victor 1420 multilabel counter; EG & G Wallac, Turku, Finland). The rate of CSF secretion was calculated as described previously (11): CSF secretion rate (μl min^{-1}) = $F_{in}(D_{in} - D_{out})/D_{out}$. D_{in} is the fluorescence of FITC-dextran in the in flow solution and D_{out} is fluorescence of FITC-dextran in the outflow solution. F_{in} is the rate of artificial cerebrospinal fluid perfusion (4 μl min^{-1}).

Measurements of Survival Rate of Animals and Brain Water Content after Acute Water Intoxication—To determine the effect of TTF-1 AS ODN on the survival rate of animals subjected to acute water intoxication, rats were given distilled water containing 1-deamino-8-D-arginine vasopressin (dDAVP, 0.4 μg/kg body weight; Sigma) equal to a 25% of body weight by intraperitoneal injection, as reported previously (24), 12 h after the second ODN injection. Beginning immediately after water injection, the survival rate of animals was monitored for 24 h. To measure brain water content (11), some animals were sacrificed 1 h after water injection, and their brains were weighed immediately and dried in a vacuum oven at 105 °C for 24 h. The dried brains were weighed again, and % brain water content was calculated as (wet weight − dry weight) × 100/wet weight.

Statistics—The differences between several groups were analyzed by analysis of variance with Dunnett's multiple comparison test. Student's *t* test was used for the comparison of two groups.

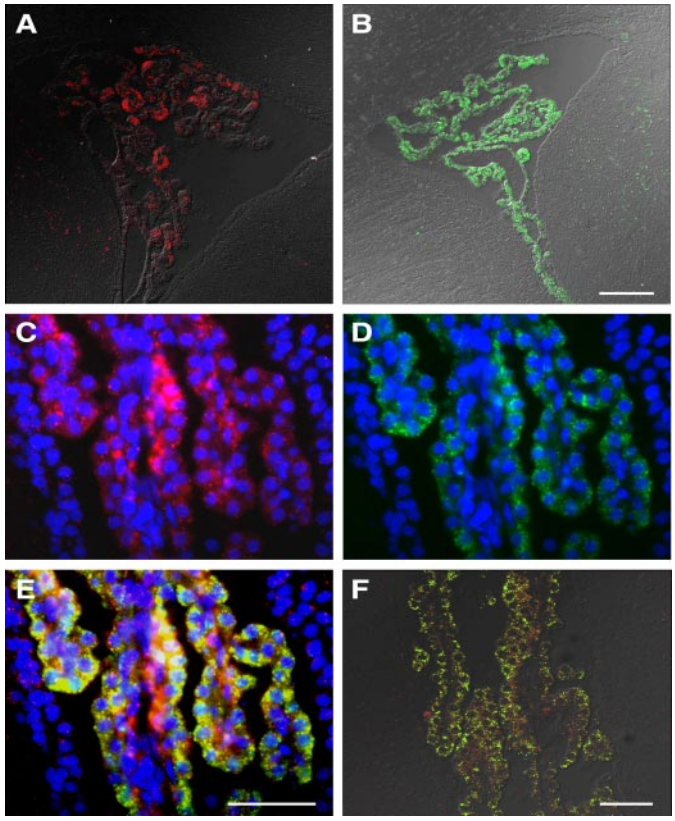

FIGURE 1. **Localization of TTF-1 and AQP-1 mRNA in choroid plexus of the lateral ventricle.** *A,* confocal microphotograph showing TTF-1 mRNA identified by hybridization to a digoxygenin-labeled TTF-1 cRNA probe and detected by Cy3-coupled tyramide. *B,* confocal microphotograph representing AQP-1 mRNA hybridized to a fluorescein-labeled AQP-1 cRNA probe and detected by FITC-coupled tyramide. *C,* fluorescence microphotograph showing TTF-1 mRNA (*red*) surrounding the nuclei (stained with Hoechst 33258, *blue color*) of choroid plexus cells. *D,* fluorescence microphotograph showing the presence of AQP-1 mRNA (*green*) in the cytoplasm of choroid plexus cells. *E,* merged image of *C* and *D*, showing colocalization (*yellow*) of TTF-1 and AQP-1 mRNAs in the cytoplasm of choroid plexus cells. *F*, confocal laser microscopic image of *E*. *Scale bar*, 200 μm in *B* and 50 μm in *E* and *F*.

RESULTS

TTF-1 and AQP-1 mRNA Are Coexpressed in the Rat Choroid Plexus—The choroid plexus is a tissue in the ventricle regions of the brain with branched structures made up of numerous villi that are composed of a single layer of epithelial cells overlying a core of connective tissue and blood capillaries (1). Previous reports have shown that AQP-1 is exclusively expressed in the apical membrane of the choroid plexus epithelium (25). We used FISH to determine the localization of TTF-1 and AQP-1 mRNAs in the choroid plexus. FISH showed that TTF-1 mRNA was expressed in epithelial cells of the lateral ventricular choroid plexus (Fig. 1, *A* and *C*, *red*), and as expected, AQP-1 was exclusively expressed in choroid plexus epithelial cells (Fig. 1, *B* and *D*, *green*). Double FISH demonstrated that TTF-1 mRNA was present in all AQP-1 mRNA-containing cells of the choroid plexus (Fig. 1, *E* and *F*, *yellow*). The donut-shaped fluorescence staining strongly revealed that both mRNA signals were present only in the cytoplasm surrounding cellular nuclei stained with Hoechst 33258 (Fig. 1, *C* and *D*). We also confirmed the colocalization of TTF-1 and AQP-1 mRNAs in the choroid plexus by classical double *in situ* hybridization using DIG-labeled

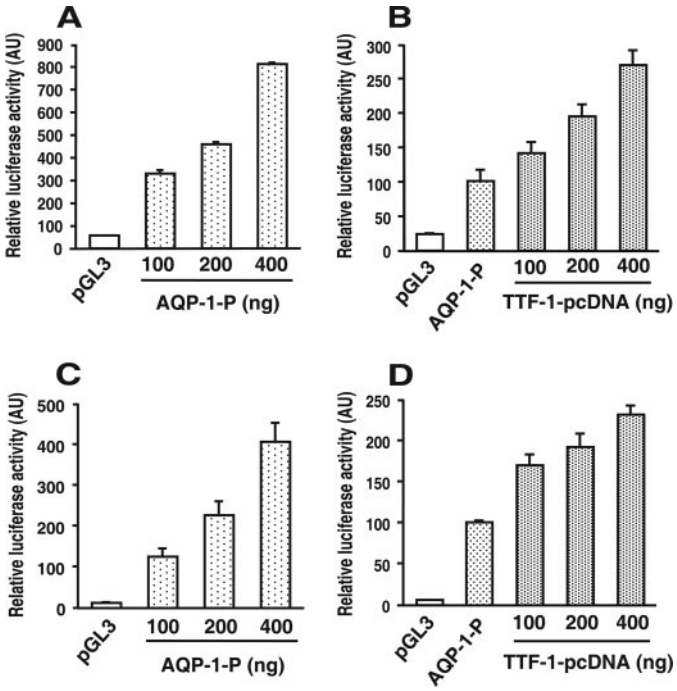

FIGURE 2. **Transactivation of the *AQP-1* gene by TTF-1.** Luciferase reporter constructs (*pGL3*) containing the 5′-flanking region of the AQP-1 gene (*AQP-1-P*) were cotransfected into BAS8.1 and C6 cells with an expression vector carrying the rat TTF-1-coding region (*TTF-1-pcDNA*) at the indicated final concentrations. The cells were harvested for luciferase and β-galactosidase assays 24 h after transfection. *A,* dose-related increase in AQP-1 promoter activity following transfection of different amounts of AQP-1-P in BAS8.1 cells. *B,* transactivation of the AQP-1 promoter by different concentrations of TTF-1 in BAS8.1 cells. *C,* dose-related increase in AQP-1 promoter activity following transfection of different amounts of AQP-1-P in C6 cells. *D,* transactivation of the AQP-1 promoter by different concentrations of TTF-1 in C6 cells. Results are the means ± S.E. of at least six wells per group. *AU*, arbitrary units.

TTF-1 cRNA and ^{35}S-UTP-labeled AQP-1 cRNA probes (data not shown). In control experiments, hybridization with DIG-labeled TTF-1 sense RNA or fluorescein-labeled AQP-1 sense RNA probes revealed absence of specific signals detected in the choroid plexus (data not shown).

TTF-1 Transactivates the AQP-1 Promoter—The coexpression of TTF-1 and AQP-1 suggested that the former may control transcription of the *AQP-1* gene. Thus, we evaluated whether TTF-1 was able to activate the AQP-1 promoter.

In this study, we used the 5′-flanking region of the human *AQP-1* gene, as no confirmed promoter sequence for mouse or rat AQP-1 has been reported to date. We also used a rat TTF-1 expression vector to transfect either mouse BAS8.1 glial progenitor cells or rat glioma C6 cells, both of which express AQP-1 mRNA detected by RT-PCR (data not shown). Rat TTF-1 is expected to be biologically active across species because there is more than 96% sequence homology at the amino acid level between human, mouse, and rat TTF-1. Accordingly, functional analysis of the AQP-1 promoter demonstrated that this promoter was transcriptionally active over a wide range of concentrations in both cell lines (Fig. 2, *A* and *C*). Moreover, when AQP-1 promoters were cotransfected with a TTF-1 expression vector, the AQP-1 transcriptional activity was dramatically increased in a dose-dependent manner in both cell lines (Fig. 2, *B* and *D*).

TABLE 1
EMSA oligonucleotide probes
Each sequence represents the sense strand of probes; core TTF-1 binding motifs are underlined. * and + denote positive and negative control probes, respectively (see text).

Location in the 5′-flanking region of *AQP-1* gene	Probe sequences
C*	5′-CACTGCCCAT**CAAG**TGTTCTTGA-3′
Cβ+	5′-CACTGCCCAGTCACGCGTTCTTGA-3′
−1732	5′-CAGGCAGGGCC**CTTG**GGCCACCAC-3′
−1635	5′-GCAATTCACCC**CAAG**AGCCAGGCC-3′
−1560	5′-GCCCCTGGA**CAAG**AGGCATAAG-3′
−1533	5′-CCCACTCATC**CTTG**CCCTGCCCC-3′
−1324	5′-CATGCAGCAGG**CAAG**AGGGCCAGG-3′
−1291	5′-CCTGACAG**CTTG**CTGGCCCTG-3′
−1267	5′-GTCCAGATT**CTTG**TTTGTTGGCTG-3′
−1112	5′-CTTTCTGCTT**CTTG**GCTCTGGGTC-3′
−1027	5′-CTCAGCCCTG**CTTG**TCTCACTGTC-3′
−943	5′-CTTTCTC**CTTG**TCTGTCTCTTCTC-3′
−793	5′-GTGTGACTGC**CTTG**AGAGGAAAG-3′
−724	5′-CAAATCGCT**CTTG**AGAAGTTTGGG-3′
−516	5′-CGGGAGGA**CTTG**ACTGCCCCTCTG-3′
−273	5′-GTGGGGCCAG**CTTG**GAAGAATTTC-3′

Transient transfection of C6 cells with TTF-1 expression vectors (400 ng/ml) resulted in a 2-fold increase in TTF-1 protein content, which was comparable with that detected in protein extracts from the rat choroid plexus (data not shown). Thus, the levels of TTF-1 protein achieved after transient transfection of a TTF-1 producing plasmid can be considered as being within a physiological range.

TTF-1 Binds to Several Putative Binding Sites in the 5′-Flanking Region of the AQP-1 Gene—It is known that TTF-1 is able to bind at high affinity sequences containing the 5′-CAAG-3′ core motif (19). Thus, to find TTF-1-binding sites in the AQP-1 promoter, we subjected all sequences of AQP-1 promoter containing the 5′-CAAG-3′ core motif to EMSA analysis. Double-stranded oligodeoxynucleotide probes (Table 1) containing TTF-1-binding sites and their flanking sequences were employed. Of the 14 putative binding sites, 12 were recognized by TTF-1 HD (Fig. 3*A*). The probes containing binding sites at −1732, −1635, −1560, −1324, −793, −724, and −516 showed a relatively high binding activity (Fig. 3*B*), >50% of the binding activity displayed by TTF-1 HD binding to site C of thyroglobulin promoter, used as a positive control (20), whereas the sites at −1533, −1267, −1112, −1027, and −943 had much lower binding activity. The sites at −1291 and −273 had no binding activity, and thus were not be considered as true TTF-1-binding sites. These data confirm previous findings (19), demonstrating that the presence of the 5′-CAAG-3′ core motif alone is not sufficient for TTF-1 high affinity binding. Interestingly, the presence of a cytosine at position +1 with respect to the 5′-CAAG-3′ core motif seemed to have a detrimental effect on TTF-1 binding. This arrangement was seen in probes −1291 and −273 (Table I), which had no TTF-1 binding activity, and in probe −1027, which exhibited reduced TTF-1 binding activity.

To test whether, in choroid plexus cells, TTF-1 is present in a configuration able to specifically interact with the AQP-1 promoter, EMSAs were performed with nuclear extracts from the rat choroid plexus, using probe −724 that showed the strongest binding capability (Fig. 3, *A* and *B*). Nuclear proteins from the rat choroid plexus strongly bound to the −724 oligonucleotide probe (Fig. 3*C*). The interaction of the labeled probe with cho-

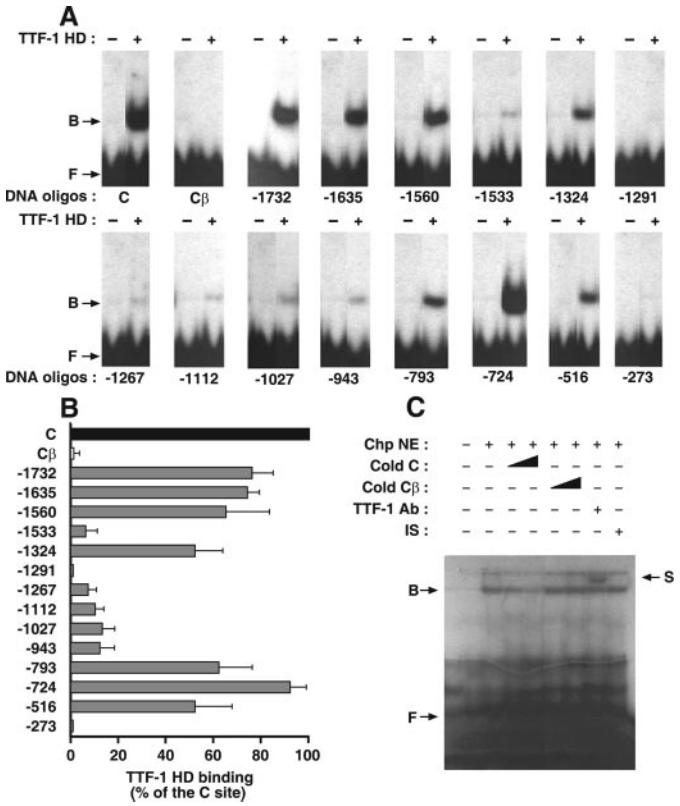

FIGURE 3. **EMSAs.** EMSAs were performed with double-stranded oligomer probes containing the putative TTF-1-binding core motifs shown in Table 1. *A,* representative autoradiograms showing binding of TTF-1 HD to putative TTF-1-binding sites in 5′-flanking region of the *AQP-1* gene. The DNA probes and TTF-1 HD were used at a final concentration of 5 mM and 150 nM, respectively. *B,* relative binding activities calculated as a percentage of TTF-1 HD binding to probe C. Each *bar* represents the mean value derived from three different EMSAs. *C,* choroid plexus nuclear extracts (*Chp NE*) were incubated with oligonucleotide probe (−724), in the presence (+) or absence (−) of 5- or 20-fold excess of cold oligonucleotide C or C*β* and TTF-1 antibody (*Ab*) or preimmune serum (*IS*). Incubation of nuclear proteins with a TTF-1 antibody prior to the protein-DNA binding reaction delays (*arrow S*, supershift) the migration of the protein-DNA complex. *B*, protein-bound DNA; *F*, free DNA; *S*, supershifted DNA.

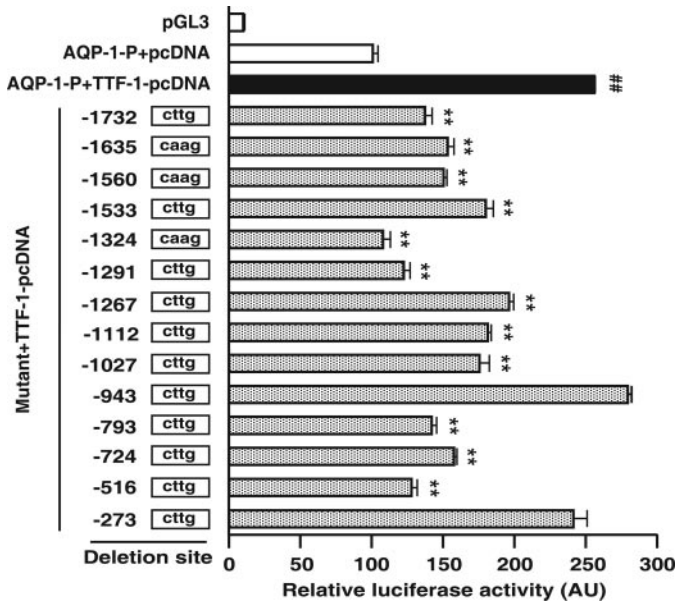

FIGURE 4. **Effect of site-specific deletion of core TTF-1-binding motifs on the transactivation of the AQP-1 promoter (*AQP-1-P*) by TTF-1.** Fourteen single mutants with core TTF-1-binding motifs deleted were cotransfected with 400 ng of the TTF-1 expression vector (*TTF-1-pcDNA*). The positions of the deleted binding sites are indicated. The data are means ± S.E. of six wells per construct. ##, $p < 0.01$ *versus* AQP-1-P + pcDNA; **, $p < 0.01$ *versus* AQP-1-P + TTF-1-pcDNA. *AU*, arbitrary units.

roid plexus nuclear proteins was reduced by addition of a 5- or 20-fold excess of unlabeled oligonucleotide C. In contrast, an oligonucleotide carrying a mutated core TTF-1-binding sequence C (C*β*) unable to bind TTF-1 (20) was ineffective. Preincubation of choroid plexus nuclear proteins with a TTF-1 antibody delayed the migration of the protein-DNA complex, indicating that TTF-1 was indeed part of this complex.

Loss of AQP-1 Transactivation by TTF-1 after Deletion of TTF-1 Binding Core Motifs—To determine whether the 12 binding sites of TTF-1 recognized by EMSAs are functionally active, we deleted each of 5′-CAAG-3′ motifs by site-directed mutagenesis, and we examined the ability of TTF-1 to transactivate the mutated promoters in BAS8.1 cells. As shown in Fig. 4, deletion of each site having a high TTF-1 binding activity (−1732, −1635, −1560, −1324, −793, −724, and −516) resulted in the significant reduction of the TTF-1-induced upregulation of the AQP-1 promoter. Deletion at site −1324 completely abolished TTF-1 action. In agreement with EMSA results, deletion of the 5′-CAAG-3′ motif at position −273 (to which TTF-1 is unable to bind, Fig. 3) had no effect on TTF-1 action. However, deletion of the other 5′-CAAG-3′ motif, which is not recognized by TTF-1 (−1291; see Fig. 3), resulted in the almost complete abolition of TTF-1 action. Therefore, in this case the deletion caused a transcriptional effect that was independent of TTF-1 binding. Among binding sites that display a relatively low binding affinity for TTF-1 (−1533, −1267, −1112, −1027, and −943), deletion at position −943 had no effect on TTF-1 action. Deletions at other low affinity TTF-1-binding sites caused intermediate reduction of the TTF-1 effect. Altogether, it appears that the *AQP-1* gene promoter has multiple TTF-1-binding sites and that deletion of each of them is able to reduce the transcriptional effect of TTF-1. In fact, with the exception of the site at position −943, deletion of any of the TTF-1-binding sites identified by EMSA affected transcriptional activity. On the other hand, among the sites that did not exhibit TTF-1 binding in EMSA, deletion at site −1291 had a dramatic effect on TTF-1 action, suggesting that TTF-1 may require other transcriptional activators binding to this site to enhance *AQP-1* gene transcription.

Effect of an AS TTF-1 ODN on AQP-1 mRNA and Protein Levels in the Choroid Plexus—To determine whether *in vivo* blockade of TTF-1 expression decreased AQP-1 synthesis in the choroid plexus, we injected a TTF-1 AS ODN or a scrambled (SCR) sequence into the lateral ventricle of 2-month-old male rats (for details see "Experimental Procedures"), and we examined the choroid plexus for TTF-1 protein and AQP-1 mRNA and protein 12 h after the second ODN injection. As shown in Fig. 5*A*, the AS ODN injection effectively decreased the content of TTF-1 protein in the choroid plexus, as determined by Western blot analysis. This reduction in TTF-1 protein levels was accompanied by a reduction in AQP-1 mRNA abundance (detected by real time PCR; Fig. 5*B*) and AQP-1 protein (detected in Western blots; Fig. 5*C*). Thus, TTF-1

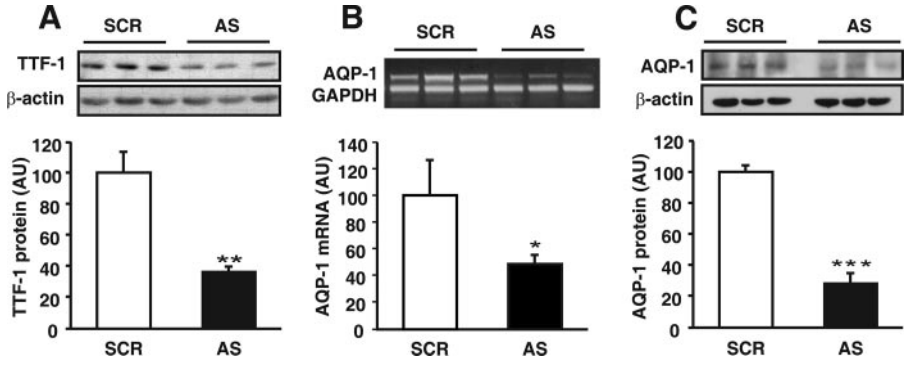

FIGURE 5. **Effect of TTF-1 synthesis blockade by an AS TTF-1 ODN on AQP-1 synthesis in the rat choroid plexus.** TTF-1 AS ODN or an SCR sequence of identical base composition was injected into the lateral ventricle. One day after the ODN injection, RNA and protein were extracted from the choroid plexus, and levels of TTF-1 and AQP-1 protein and AQP-1 mRNA were determined by Western blot and real time PCR analysis, respectively. *A,* Western blots showing a decrease in TTF-1 protein caused by AS TTF-1 ODN (*AS*) administration. *B,* AS ODN significantly decreased AQP-1 mRNA level compared with the SCR ODN-injected groups (*SCR*). *C,* Western blots showing the effectiveness of TTF-1 AS ODN in decreasing AQP-1 protein content in the choroid plexus. Data are represented as means ± S.E. ($n = 5$). *AU*, arbitrary units. *, $p < 0.05$; **, $p < 0.01$; ***, $p < 0.001$ *versus* control SCR ODN-injected group.

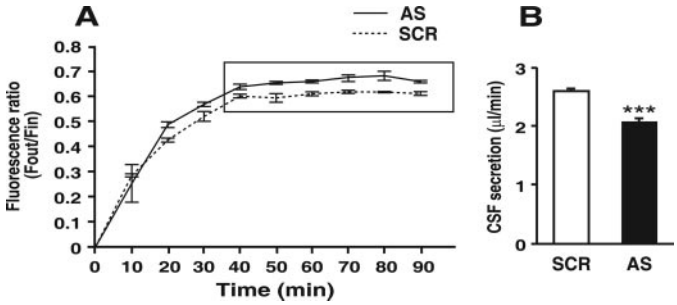

FIGURE 6. **Effect of TTF-1 synthesis blockade on CSF formation.** CSF formation was measured by a ventriculocisternal perfusion method (see text for details) after an intracerebroventricular injection of TTF-1 AS ODN or SCR ODN. *A,* effect of AS ODN on FITC-dextran recovery (F_{out}/F_{in}) from CSF throughout a 90-min ventriculocisternal perfusion. FITC-dextran was infused into the lateral ventricle of rats treated with ODNs at a rate of 4 μl min^{-1}. CSF was collected from the cisterna magna beginning immediately after infusion. *B,* effect of AS ODN on CSF secretion. The rate of CSF secretion was calculated from the CSF samples collected after the fluorescence ratio (F_{out}/F_{in}) achieved steady-state levels (*inset* in *A*). Data are represented as means ± S.E. ($n = 5$). ***, $p < 0.001$ *versus* SCR ODN-injected controls.

appeared to sustain AQP-1 gene expression *in vivo* as well as in cell lines *in vitro*.

We performed relative RT-PCR analysis of some mRNA species using gene-specific primer sets to verify the possible involvement of other proteins such as ion transporters and AQP-4, which could be potentially involved in the CSF formation (1), in the TTF-1 AS ODN-induced decrease in CSF formation (see Fig. 6 in detail). Ion transporters used in this experiment included Na^+-K^+-ATPase, Na^+-H^+ exchange, K^+-Cl^- cotransporter, Cl^--$HCO3^-$ exchange, Kv channel, and Kir channel, which have all been demonstrated to be expressed in the choroid plexus and are involved in the CSF secretion through creation of an osmotic gradient (1).

Although no significant change was found in the expression of any of these ion transporters, abundance of AQP-4 mRNA was significantly decreased (data not shown). Although evidence that AQP-4 is involved in CSF formation is still lacking, it appears entirely possible (1, 10). Therefore, we focused on the TTF-1-dependent AQP-1 function for the CSF formation in this study.

Effects of AS TTF-1 ODN on CSF Formation—To determine whether TTF-1 is required for CSF formation, impermeable FITC-dextran was perfused into the lateral ventricle of the rat brain after an injection of AS or SCR ODN, and CSF was collected from the cisterna magna. Fluorescence levels in the perfusate (F_{in}) and collected CSF (F_{out}) at different times after the injection were determined by fluorimetric analysis. As shown in Fig. 6*A*, the fluorescence ratio (outflow/inflow) reached a steady state ~40 min after initiation of the perfusion and remained unchanged thereafter. FITC-dextran cannot be transported out of the ventricular system and is therefore diluted by newly synthesized CSF. Accordingly, the formation of CSF can be calculated by subtracting outflow (F_{out}) from inflow fluorescence values (F_{in}) (see "Experimental Procedures" for details). As shown in Fig. 6*B*, the average CSF production rate in SCR ODN-injected control rats was 2.59 μl min^{-1} ($n = 5$). This rate was significantly decreased by TTF-1 AS ODN injection (2.07 μl min^{-1}; $n = 5$, $p < 0.001$).

Survival after Brain Edema and Brain Water Content of Animals Injected with TTF-1 AS ODN—Experiments were performed to determine whether inhibition of TTF-1 synthesis affects brain water content and the survival rate of animals with brain edema induced by acute water intoxication. Twelve hours after an intraventricular injection of TTF-1 AS ODN or SCR ODN, rats received an intraperitoneal injection of distilled water (25% body weight) containing dDAVP, which has a strong antidiuretic effect. Many of the SCR ODN-injected rats became comatose and died within 3 h of the water-dDAVP injection. By 3 h, only 28.6% of the SCR ODN-injected rats were alive, whereas 85.7% of the TTF-1 AS ODN-injected rats remained alive until end of the experiment (12 h) (Fig. 7*A*). Total brain water content measured 1 h after the water-dDAVP injection was similarly increased in both AS ODN and SCR ODN-injected groups (Fig. 7*B*).

DISCUSSION

AQP-1 plays an important role in the regulation of body fluid movement, such as formation of urine in the renal medulla, production of CSF in the brain, and secretion of aqueous humor in the eye (26–28). It is now known that AQP-1 synthesis is regulated by several intracellular pathways, including a cAMP-dependent pathway that operates under physiological conditions (29), and ERK, p38 kinase, c-Jun NH_2-terminal kinase (JNK), and the hypertonicity response element pathways, all of which are regulated by hypertonicity (28, 30). Evidence also exists that AQP-1 synthesis is regulated by retinoic acid and glucocorticoids in human erythroleukemia cells (31, 32). Despite the wealth of information for AQP-1, little if anything is know about the upstream transcriptional factor that regulates *AQP-1* gene expression.

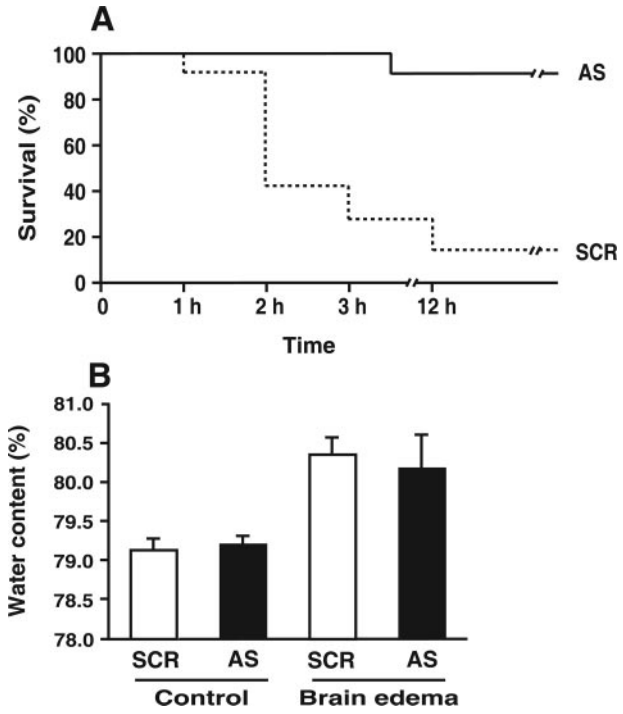

FIGURE 7. **Survival rate and tissue water content after acute water intoxication in animals injected with either TTF-1 AS ODN or SCR ODN.** *A,* effect of water intoxication on survival rate of rats treated with TTF-1 AS ODN and SCR ODN. Twelve hours after ODN injection, rats received an intraperitoneal injection of distilled water (25% body weight) containing dDAVP (seven animals per group). *B,* change in total brain water content induced by water injection. Brain water content was measured 1 h after water injection. Data are presented as means ± S.E.

We now report that TTF-1, a homeodomain protein of the Nkx family of transcriptional regulators (13), directly regulates *AQP-1* gene transcription in the choroid plexus of the rat brain. Our *in situ* hybridization results revealed that TTF-1 and AQP-1 mRNA were colocalized in most of the epithelial cells of the choroid plexus, suggesting that both genes may also share a functional relationship in this highly specialized region of the brain. An early indication that this relationship is physiologically relevant was provided by the microarray-derived observation that mutations of TTF-1 phosphorylation sites resulted in a significant decrease in AQP-1 mRNA content in the mouse lung (33).

In earlier studies we have found that TTF-1 targets several downstream genes for regulation in the neuroendocrine brain, including the luteinizing hormone-releasing hormone, proenkephalin, ErbB-2, pituitary adenylate cyclase-activating polypeptide, and angiotensinogen genes (15, 17, 18). Identification of these target genes was initially suggested by two findings as follows: first, the cellular colocalization of TTF-1 mRNA with the mRNAs encoded by each of the putative target genes, and second, the presence of conserved TTF-1-binding motifs in their 5′-flanking regions. This approach has again been proven to be fruitful in the present study. Because high affinity TTF-1-binding sites are strictly conserved in TTF-1 target genes and the 5′-flanking region of the AQP-1 gene has 14 5′-CAAG-3′ core motifs of TTF-1 binding, we performed TTF-1 binding activity analysis of these 14 potential sites. We found that 12 sites recognize the TTF-1 HD, with 7 sites able to bind with high affinity. Single deletion of the core binding motifs in each of the 12 positive sites resulted in a reduced TTF-1-dependent increase in AQP-1 promoter activity, strongly suggesting that TTF-1 directly transactivates the AQP-1 gene by binding to a multiplicity of recognition sites.

The finding that the AQP-1 promoter contains so many functional TTF-1-binding sites is not surprising. In fact, the existence of a relatively high number of binding sites for a single transcription factor in a transcriptional unit has already been described for TTF-1 (34) as well as other transcriptional activators (35, 36). Fig. 4 shows that most of the TTF-1-binding sites identified by EMSA also had a functional role as determined by promoter assays. A possible explanation for this finding is simple; the activation of the AQP-1 promoter requires an "efficient" interaction between TTF-1 and the promoter; this is reached by the presence of multiple binding sites.

It is believed that transcription factors reach their target genes by three-dimensional diffusion as well as "sliding" on the DNA double helix (37). According to this view, a protein contacts DNA with low affinity, quickly scans a DNA segment by sliding on it, and then hops to other loci until it finds a target site. Low affinity sites may slow down the protein sliding process as the corresponding transcription factor approaches the high affinity site and could help to enrich the local concentration of the protein. Thus, this model could explain the finding of multiple functional TTF-1-binding sites (some of them with a relatively low binding affinity) on the AQP-1 promoter. The recent observation that degenerate transcription factor binding sites are enriched around cognate nondegenerate binding sites also supports this view (38).

To determine whether these molecular interactions between TTF-1 and its multiple binding sites in the AQP-1 promoter reflect the existence of a physiological role for TTF-1 in the control of AQP-1 synthesis in the choroid plexus, and considering that the main function of AQP-1 in this region of the brain is to maintain CSF production (1), we examined the changes in CSF production, resulting from selectively interfering with TTF-1 synthesis in the choroid plexus. Epithelial cells of the choroid plexus are responsible for secreting the majority of CSF into the ventricular system of the brain. The process of CSF secretion includes the precisely regulated transport of Na^+, Cl^-, and HCO_3^- from the bloodstream into the ventricles, creating an osmotic gradient that drives secretion of water into the ventricular compartment (1). AQP-1 is selectively present in the apical membrane of choroid plexus epithelial cells, which serves a pathway for water diffusion by osmotic gradients (39, 40). More direct evidence for the role of AQP-1 in CSF secretion has been reported recently, as CSF production is reduced in AQP-1-deficient mice by ~20% (11, 27). Our results demonstrate that blockade of TTF-1 synthesis markedly reduced AQP-1 synthesis in the choroid plexus and decreased CSF formation by ~20%. It would then appear that control of *AQP-1* gene transcription by TTF-1 is a major mechanism underlying the production of CSF in brain.

The capacity of CSF and venous compartments to constrict is critical for the brain to resist a rise in ICP caused by an increase in brain parenchyma volume (41). For example, ICP is strongly augmented by a small increase in CSF volume (42). Moreover, it

has been suggested that the reduction of ICP seen in AQP-1-deficient mice is because of decreased CSF formation. Accordingly, AQP-1 deficiency provides a survival advantage to animals subjected to an increase in ICP (11). Our results support this concept by showing that animals in which AQP-1 synthesis is reduced by blockade of TTF-1 expression survive longer and in greater numbers than AQP-1 intact rats.

In the acute water intoxication model we used, a rapid intraperitoneal water infusion causes an abrupt decrease in serum osmolality, which creates an osmotic gradient driving water influx into the brain (24). Thus, the infused water causes cytotoxic edema without disrupting the blood-brain barrier. During this acute phase, ICP increases, resulting in brain swelling with a substantially increased mortality rate (11, 24). Our data show that TTF-1 synthesis blockade significantly improved the survival rate of animals subjected to acute water intoxication-induced brain edema. Despite the robustness of this effect, brain water content was not altered, suggesting that the improved survival rate was not because of a detectable reduction in brain water content caused by the AS ODN-induced loss of TTF-1. Instead, the underlying mechanism may involve a decreased secretion of CSF resulting from the loss of AQP-1 caused by the inhibition of TTF-1 synthesis. This reduction would, in turn, cause a decrease in ICP, resulting in increased survival rate, as reported previously to occur in AQP-1 null mice (11). A small increment in CSF volume can cause a large change in ICP (11), particularly following brain edema, because brain compliance is nonlinear (42).

Elevation of ICP can result from several neurological conditions such as hydrocephalus, traumatic brain injury, and hyponatremia. Without prompt treatment death becomes inevitable. Current clinical treatment for cerebral edema includes administration of intravenous hypertonic solutions, removal of damaged tissue, and drainage of CSF. Each one of these procedures is aimed at reducing ICP; however, they are not without undesirable side effects, making their use of limited value (43, 44). It has recently been suggested that inhibition of AQP-1 synthesis might be an effective means of lowering ICP (11). Our results suggest that a novel approach to reduce elevated ICP might be found in agents able to inhibit brain AQP-1 synthesis at the transcriptional level.

REFERENCES

1. Brown, P. D., Davies, S. L., Speake, T., and Millar, I. D. (2004) *Neuroscience* **129,** 957–970
2. Segal, M. B. (1993) *J. Inherit. Metab. Dis.* **16,** 617–638
3. Johanson, C. E., Preston, J. E., Chodobski, A., Stopa, E. G., Szmydynger-Chodobska, J., and McMillan, P. N. (1999) *Am. J. Physiol.* **276,** C82–C90
4. Venero, J. L., Vizuete, M. L., Machado, A., and Cano, J. (2001) *Prog. Neurobiol.* **63,** 321–336
5. Arima, H., Yamamoto, N., Sobue, K., Umenishi, F., Tada, T., Katsuya, H., and Asai, K. (2003) *J. Biol. Chem.* **278,** 44525–44534
6. Gunnarson, E., Zelenina, M., and Aperia, A. (2004) *Neuroscience* **129,** 947–955
7. Papadopoulos, M. C., and Verkman, A. S. (2005) *J. Biol. Chem.* **280,** 13906–13912
8. Umenishi, F., Verkman, A. S., and Gropper, M. A. (1996) *DNA Cell Biol.* **15,** 475–480
9. Preston, G. M., and Agre, P. (1991) *Proc. Natl. Acad. Sci. U. S. A.* **88,** 11110–11114
10. Speake, T., Freeman, L. J., and Brown, P. D. (2003) *Biochim. Biophys. Acta* **1609,** 80–86
11. Oshio, K., Watanabe, H., Song, Y., Verkman, A. S., and Manley, G. T. (2005) *FASEB J.* **19,** 76–78
12. Civitareale, D., Lonigro, R., Sinclair, A. J., and Di Lauro, R. (1989) *EMBO J.* **8,** 2537–2542
13. Guazzi, S., Price, M., De Felice, M., Damante, G., Mattei, M. G., and Di Lauro, R. (1990) *EMBO J.* **9,** 3631–3639
14. Lazzaro, D., Price, M., de Felice, M., and Di Lauro, R. (1991) *Development* (*Camb.*) **113,** 1093–1104
15. Lee, B. J., Cho, G. J., Norgren, R. B., Jr., Junier, M. P., Hill, D. F., Tapia, V., Costa, M. E., and Ojeda, S. R. (2001) *Mol. Cell. Neurosci.* **17,** 107–126
16. Nakamura, K., Kimura, S., Yamazaki, M., Kawaguchi, A., Inoue, K., and Sakai, T. (2001) *Brain Res. Dev. Brain Res.* **130,** 159–166
17. Son, Y. J., Hur, M. K., Ryu, B. J., Park, S. K., Damante, G., D'Elia, A. V., Costa, M. E., Ojeda, S. R., and Lee, B. J. (2003) *J. Biol. Chem.* **278,** 27043–27052
18. Kim, M. S., Hur, M. K., Son, Y. J., Park, J. I., Chun, S. Y., D'Elia, A. V., Damante, G., Cho, S., Kim, K., and Lee, B. J. (2002) *J. Biol. Chem.* **277,** 36863–36871
19. Damante, G., Pellizzari, L., Esposito, G., Fogolari, F., Viglino, P., Fabbro, D., Tell, G., Formisano, S., and Di Lauro, R. (1996) *EMBO J.* **15,** 4992–5000
20. Pellizzari, L., Tell, G., and Damante, G. (1999) *Biochem. J.* **337,** 253–262
21. Andrews, N. C., and Faller, D. V. (1991) *Nucleic Acids Res.* **19,** 2499
22. Kuhn, R., Monuki, E. S., and Lemke, G. (1991) *Mol. Cell. Biol.* **11,** 4642–4650
23. Davson, H., Hollingsworth, J. G., Carey, M. B., and Fenstermacher, J. D. (1982) *J. Neurobiol.* **13,** 293–318
24. Manley, G. T., Fujimura, M., Ma, T., Noshita, N., Filiz, F., Bollen, A. W., Chan, P., and Verkman, A. S. (2000) *Nat. Med.* **6,** 159–163
25. Nielsen, S., Smith, B. L., Christensen, E. I., and Agre, P. (1993) *Proc. Natl. Acad. Sci. U. S. A.* **90,** 7275–7279
26. Zhang, D., Vetrivel, L., and Verkman, A. S. (2002) *J. Gen. Physiol.* **119,** 561–569
27. Oshio, K., Song, Y., Verkman, A. S., and Manley, G. T. (2003) *Acta Neurochir.* **86,** S525–S528
28. Umenishi, F., and Schrier, R. W. (2003) *J. Biol. Chem.* **278,** 15765–15770
29. Han, Z., and Patil, R. V. (2000) *Biochem. Biophys. Res. Commun.* **273,** 328–332
30. Umenishi, F., and Schrier, R. W. (2002) *Biochem. Biophys. Res. Commun.* **292,** 771–775
31. Moon, C., King, L. S., and Agre, P. (1997) *Am. J. Physiol.* **273,** C1562–C1570
32. Umenishi, F., and Schrier, R. W. (2002) *Biochem. Biophys. Res. Commun.* **293,** 913–917
33. DeFelice, M., Silberschmidt, D., DiLauro, R., Xu, Y., Wert, S. E., Weaver, T. E., Bachurski, C. J., Clark, J. C., and Whitsett, J. A. (2003) *J. Biol. Chem.* **278,** 35574–35583
34. Ray, M. K., Chen, C. Y., Schwartz, R. J., and DeMayo, F. J. (1996) *Mol. Cell. Biol.* **16,** 2056–2064
35. Kumbrink, J., Gerlinger, M., and Johnson, J. P. (2005) *J. Biol. Chem.* **280,** 42785–42793
36. Kramer, S. G., Jinks, T. M., Schedl, P., and Gergen, J. P. (1999) *Development* (*Camb.*) **126,** 191–200
37. Halford, S. E., and Marko, J. F. (2004) *Nucleic Acids Res.* **32,** 3040–3052
38. Zhang, C., Xuan, Z., Otto, S., Hover, J. R., McCorkle, S. R., Mandel, G., and Zhang, M. Q. (2006) *Nucleic Acids Res.* **34,** 2238–2246
39. Wu, Q., Delpire, E., Hebert, S. C., and Strange, K. (1998) *Am. J. Physiol.* **275,** C1565–C1572
40. Masseguin, C., Corcoran, M., Carcenac, C., Daunton, N. G., Guell, A., Verkman, A. S., and Gabrion, J. (2000) *J. Appl. Physiol.* **88,** 843–850
41. Papadopoulos, M. C., Krishna, S., and Verkman, A. S. (2002) *Mt. Sinai J. Med.* **69,** 242–248
42. Marmarou, A., Shulman, K., and Rosende, R. M. (1978) *J. Neurosurg.* **48,** 332–344
43. Cadnapaphornchai, M. A., and Schrier, R. W. (2000) *Am. J. Med.* **109,** 688–692
44. Griesdale, D. E., and Honey, C. R. (2004) *Surg. Neurol.* **61,** 418–421

Thyroid Transcription Factor-1 Facilitates Cerebrospinal Fluid Formation by Regulating Aquaporin-1 Synthesis in the Brain

Jae Geun Kim, Young June Son, Chang Ho Yun, Young Il Kim, Il Seong Nam-goong, Jun Heon Park, Sang Kyu Park, Sergio R. Ojeda, Angela Valentina D'Elia, Giuseppe Damante and Byung Ju Lee

J. Biol. Chem. 2007, 282:14923-14931.
doi: 10.1074/jbc.M701411200 originally published online March 19, 2007
